RSC Advances

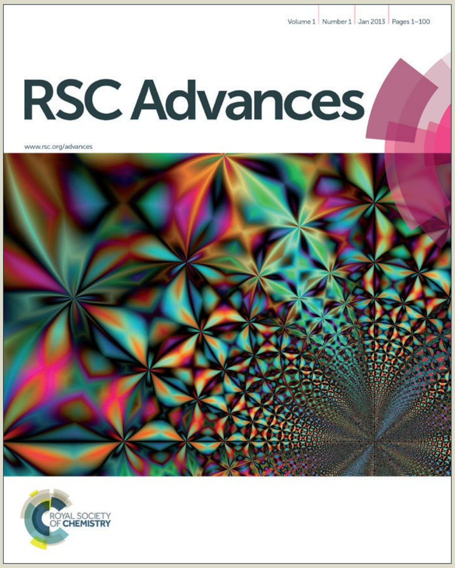

ROYAL SOCIETY OF CHEMISTRY

www.rsc.org/advances

Dynamic Article Links ►

Cite this: DOI: 10.1039/c0xx00000x

www.rsc.org/xxxxxx

PAPER

Research on Thermoplastic Starch and Different Fibers Reinforced Biomass Composites

Cheng-zhao Wang, Fang-yi Li*, Li-ming Wang, Jian-feng Li, An-fu Guo, Chuan-wei Zhang, Peng Liu

Received (in XXX, XXX) Xth XXXXXXXXX 20XX, Accepted Xth XXXXXXXXX 20XX

DOI: 10.1039/b000000x

Abstract: Thermoplastic starch (TPS) from native corn starch was prepared using different mass ratios of formamide-urea compound plasticizers. The influence of the compound plasticizer on hydrogen bonds has been analyzed by IR spectroscopy. The characterization of TPS was studied using X-ray diffractometry and differential scanning calorimetry. The results showed that the optimal mass proportion of starch/formamide/urea was 10/2/1. Starch plasticization destroyed the crystal structure of the native starch, increased the melting point of starch and improved the processability. Scanning electron micoroscope showed that there was significant change between starch molecules before and after plasticization. With the best plasticizing proportion of formamide-urea compound plasticizers, four kinds of thermoplastic starch composites reinforced with equal amount of sisal, pulp, straw and wood fibers were obtained by foam molding process. The IR spectroscopy investigations revealed the presence of hydrogen bonds and explored the mechanism of physical interactions in composites. Thermogravimetric analysis demonstrated that sisal fiber composites had the best thermal stability. Besides, the mechanical properties of different fibers reinforced composites were investigated. The sisal fiber composites demonstrated the best tensile and compressive strength, respectively, 3.85MPa and 1.37MPa among the specimens. The fracture surfaces of these composites were also observed by SEM.

1. Introduction

As one of the green materials, natural fiber-reinforced biomass composites are prepared through foam molding process. These composites have gained extensive research attention due to their attractive points such as wide bio-sources, simple preparation and environmental friendliness.

As the main ingredient of composites, plant fiber and native starch have few interactions in natural condition. However, the preprocessed plant fiber and starch have a strong interaction in composites obtained by foam molding process, which is attributed to the formation of hydrogen bonds. For untreated plant fibers, some hydroxyls in the chain molecule form hydrogen bonds; while the others are still free in the amorphous regions of cellulose.[1] The surfaces of cellulose with a negative charge could attract hydrated cations in alkaline solution. So, alkaline treatment of plant fibres accelerates the imbibition of cellulose, breaks hydrogen bonds and increases free hydroxyls. Meanwhile basic hydrolysis of cellulose leads to part glycosidic bonds fracture, forming a new reducing end and increasing free hydroxyls during the alkaline treatment. The native starch does not have thermal reprocessing ability because its crystallinity is commonly 15%~45%.[2] Plasticizers could destroy the crystal structure of native starch. The better plasticizing effect, the more free hydroxyls of thermoplastic starch (TPS) there are. Therefore, there are amounts of free hydroxyls in the preprocessed plant fiber and starch. Many scientific researches have been carried out in regard to this phenomenon. J.L.Guimaraes and F.Wypych[3] studied banana fiber reinforced starch composites and bagasse fiber reinforced starch composites, respectively. They found that the combination of bagasse fiber and thermoplastic starch was better and the composites tensile strength was closely related to the preparation process. N.P.G. Suardana, etc.[4] utilized FT-IR to characterize the chemically modified fibers. Besides, they did not find the effect of silane on the transmittance bands due to the reaction between the silane and chemical components were weak. Bogdan Jurca, etc.[5] found the presence of amorphous starch and crystalline ZnO in the ZnO–starch composites. Yanfang Xie, etc.[6] demonstrated that the stronger hydrogen bonds were formed between glycerol and starch, compared with intra- and intermolecular hydrogen bonds in native starch. Gang Li, etc.[7-8] studied the influence of the mass ratio of fiber to starch, content of plasticizer, active agent, and foaming agent on the compressive strength of biomass cushion packaging materials. They found that the content of plasticizer and the mass ratio of fiber to starch had the largest impact on the compressive strength. The common starch plasticizer was formamide, urea, glycerol and glycol.[9-12] Recent studies demonstrated that compound plasticizers, such as formamide-urea compound plasticizer, formamide-urea-glycerol compound plasticizer and glycerol-glycol compound plasticizer, had better performance in plasticizing starch than single plasticizer.[13-14] As can be concluded from the papers above, scholars mostly focused on physical-chemical properties and preparation, lack of theoretical analysis about the hydrogen bonds changing mechanism. FT-IR was just used to study the fibers or thermoplastic starch. Besides, the compound plasticizers still needed a further study on the interaction mechanism between thermoplastic starch matrix and pre-treated plant fibers.

This paper shifted infrared spectrometry from thermoplastic starch to the biomass composites for the first time. The IR spectroscopy investigations revealed the optimal plasticization proportion of formamide-urea compound plasticizer and the presence of hydrogen bonds. The characterization of TPS was studied using X-ray diffractometry and differential scanning calorimetry. The mechanism of hydrogen bonds in composites has been analyzed by IR spectroscopy, as well as the thermogravimetric analysis and mechanical performances of four kinds of fibers reinforced biomass composites. The surface morphologies of biomass composites were also observed using SEM.

2. Experimental

2.1 Materials and equipments

Materials: Sisal fiber, Straw fiber, Pulp fiber, Wood fiber, average length 6-10mm, self-made; Corn starch, reagent grade, average particle diameter about 70nm, purchased from Hebei Huachen Starch Sugar Co., Ltd; Filling: Talcum powder, 400mesh, purchased from Quanzhou Xufeng powder material Co., Ltd; Plasticizing agent: Formamide and Urea, plasticizers, AR, purchased from Tianjin Fuyu Fine Chemical Co., Ltd; Adhesive: Polyvinyl alcohol (PVA), purity≥99.0%, purchased from Sinopharm Chemical Reagent Co., Ltd; Mold-releasing agent: Steric Acid, AR, purchased from Tianjin Guangcheng Chemical Co., Ltd; NaOH, AR, purchased from Yantai Shuangshuang Chemical Co., Ltd.

The main experimental equipments in this paper were shown in Table. 1.

Table. 1 The experimental equipments

Equipments	Specification
Hot-embossing machine with double column, thermoforming mold	Custom-made
Electronic constant temperature water bath	HHS-2
Precision by force electric mixer	JJ-1
Electronic Balance	JM-B
Electric thermostat blast drying oven	DHG
FT-IR Spectrometer,	VERTEX-70
Electronic tensile machine	XLW(L)-PC
Carton compression testing machine	XYD-15K
Scanning electron microscopy	FEG250

2.2 Thermoplastic starch preparation

The constant temperature of the water bath was set to 75-85□. 100g corn starch and 300g of distilled water were mixed in the beaker under the water bath. Plasticizer (formamide-urea) was added in with the proportion (starch/formamide/urea) of 10/1/2, 10/2/2, 10/2/1 and 10/3/1 respectively. Starch plasticization could be completed after 30 minutes' churning. Distilled water played an important role in starch gelatinization, where the structure of starch granules was disordered when heated in water.[15]

2.3 Biomass composites preparation

The ingredients of biomass composites were prepared according to Table. 2.

Table. 2 Biomass composite components

Material	Plant fibers	Corn Starch	Water
Mass (g)	40	100	300
Material	AC Foaming Agent		Talcum
Mass (g)	0.5		10

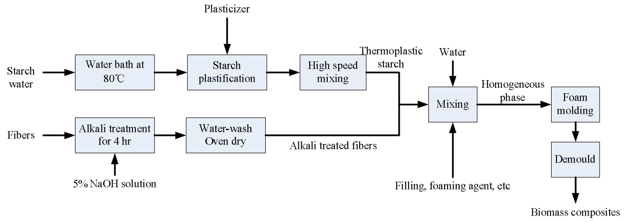

Fig. 1 Flowchart of preparation of biomass composites

In Fig. 1, the technological process of biomass composites was divided into: fiber treatment, starch plasticization, mixing and thermo-compression formation.

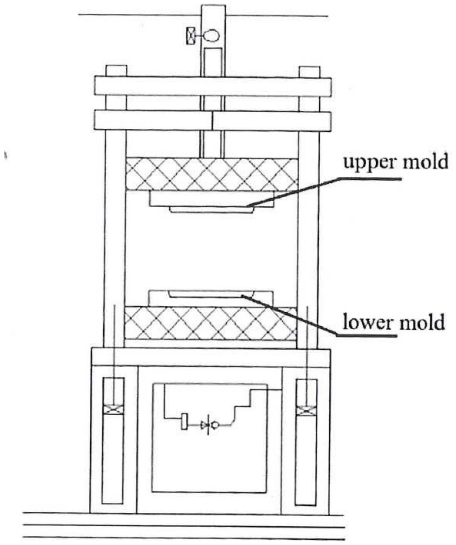

Fig. 2 Diagram of the molding machine

1) Fiber treatment: plant fibers were soaked in 5% NaOH solution for 4hr and washed with distilled water until pH reached 7. After washing, Plant fibers were kept in a hot air oven for 3hr at 90℃.

2) Starch plasticization: corn starch was mixed with water in proportion and then gelatinized in the 80℃ water bath. While churning, formamide-urea compound plasticizer was added in the starch with the optimal plasticizing mass ratio of starch/formamide/urea = 10/2/1.

3) Mixing: thermoplastic starch and treated fibers were put in churning machine. After 20-minute churning, stuffing, surfactant, foaming agent and other additives were added in and made a full mixing until homogeneous phase.

4) Thermo-compression formation (Fig. 2): the upper mold temperature was set at 220℃, lower mold at 225℃ and pressure at 4MPa. The 45g homogeneous phase was put into the lower mold. It was processed for baking of 40 s after mold close. At the stable temperature and pressure for 30 s drying, biomass composites were obtained.

2.4 The infrared spectrum analysis

After thermoplastic starch was kept in the constant temperature box for 24hr at 100℃, about 1 mg of the powder was mixed with 150 mg of KBr and milled thoroughly until the particle diameter was less than 2.5μm. This mixture was compressed into pellets under about 12-14MPa pressure and then analyzed using VERTEX-70 FT-IR Spectrometer. The spectra were recorded with a resolution of 2 cm^{-1} in the range of 400–4000 cm^{-1}.

The infrared spectroscopy test process of biomass composites was the same with the above.

2.5 Differential scanning calorimetry

Differential scanning calorimetry (DSC) was performed with a DSC DIAMOND equipment, fitted with a nitrogen gas system and a thermal analysis station. The aluminium pan hermetic pans were used to weigh the starch and TPS (about 5 mg). Sample pans were performed from room temperature to 250◦C at a heating rate of 10◦C /min. Peak temperature (Tp) of the crystal melting transition was calculated.

2.6 X-ray diffraction experiment

Thermoplastic starch was dried at 100℃ for 24 hours in order to prepare anhydrous TPS. Then, the anhydrous TPS was ground by using a agate mortar and sieved with a 200 mesh sieve. 1g sample was put into a glass sample tank. The compacted sample was flat and its surface was parallel with the glass frame. The assay was operated at room temperature by using Ni-filtered Cu radiation and a curved graphite crystal monochromator. The slit system was DS/RS/SS=1°/0.16mm/1°. The angle (2θ) interval 5-55° was analyzed at a speed of 5°/ min.

2.7 Thermogravimetric analysis

Thermogravimetric analysis of four kinds of fibers reinforced composites was carried out using TG/DTA-CRY-1 type thermal analyzer. The samples were broken with the weight from 5 to 10 mg, and heated from room temperature to 500 ◦C at a heating rate of 15 ◦C/ min in a nitrogen atmosphere.

2.8 Mechanical tests

Compressive strength experiment: test samples (100×100×25 mm) were prepared according to GB/T 8168-2008 China. As the standard method A, XYD-15K compression testing machine preloaded 5N on the specimens; the thickness of specimens was regarded as the original thickness. Then the testing machine loaded the press plate at a 12 mm/min speed along the thickness direction and recorded automatically the compression force until the specimens were crushed.

Tensile strength experiment: according to GB/T 9641-88 China, test samples (100×20×5 mm) were prepared. XLW (L)-PC electronic tensile machine tested specimens at 25mm/min speed along the length direction and measured automatically the tensile force until the specimens were fracture.

The result was the average of 5–8 specimens tested for each composite and mechanical test.

2.9 Scanning electron microscopy

The fracture surface morphologies of these composites were studied in a scanning electron microscopy FEG250 with an acceleration voltage of 10 kV. Prior to SEM observation, all samples were mounted with carbon tape on aluminium stubs and sputter coated with gold to make them conductive.

3. Results and discussion

Thermoplastic starch was a homogeneous system. And it was obtained from the strong hydrogen bond interaction between starch and plasticizer. These interactions could be identified through the FTIR spectra analysis of the blends.[16] According to the harmonic oscillator model, the reduction in force constant Δf can be represented by Eq. (1) and (2).[17]

$$\Delta f = f_p - f_{np} = \frac{\mu\left(\upsilon_{np}^2 - \upsilon_p^2\right)}{4\pi^2} \qquad (1)$$

$$\mu = \frac{m_1 \cdot m_2}{m_1 + m_2} = \frac{M_1 \cdot M_2}{\left(M_1 + M_2\right) \cdot N_A} \qquad (2)$$

where μ corresponds to the reduced mass of the oscillator, m_1 and m_2 is the mass of neighbouring chemical bonded atoms, M_1 and M_2 is the relative atomic mass, N_A is Avogadro's constant, f is the force constant and ν is the oscillating frequency. The subscripts p and np denote plasticized and non-plasticized oscillators, respectively. Some interactions are directly related to the wave number (or frequency) shift of stretching vibrations and lead to the reduction of force constant. Thus, the more the Δf changes, the stronger hydrogen bond interaction is. Also the peak frequency is up to the strength of the interaction.

In the infrared spectrum of thermoplastic starch and biomass composites, absorbance that associated with stretching oscillation exists around 3300~3645cm^{-1}. Hydrogen bonds (H-O⋯H) are easily formed between plasticizer molecules and starch molecules, with stronger interaction. Hydrogen-bonding effect obviously changes the oscillating frequencies of group O-H in the infrared spectrum, which drives the absorbance to move toward the lower frequency. Thus, the lower the wave number is, the stronger is hydrogen bond.[18]

3.1 Infrared spectrum analysis on thermoplastic starch

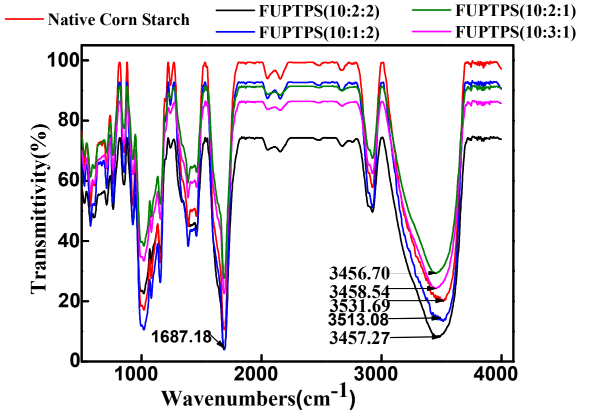

Fig. 3 The infrared spectra (FTIR) of native starch and four kinds of FUPTPS

Fig.3 illustrated changes in the frequency and absorbance in the region of O-H group vibrations of thermoplastic starch prepared by different mass radio of formamide - urea compound plasticizer. In Fig.3, it was found that the compound plasticizer drove the absorption peaks of group O-H (3531.69cm^{-1}) to move toward the lower frequency. The wave number of group O-H reduced to 3457.27, 3456.70, 3513.08, 3458.54 cm^{-1}, respectively and the minimum displacement toward lower frequency was 18.61cm^{-1}. The optimal plasticization proportion of starch/formamide/urea was 10/2/1. Experimental results showed that thermoplastic starch formed stronger hydrogen bonds.

Table. 3 Wave number of hydrogen bonds in FT-IR spectrum and the change of Δf

	Mass radio of starch / formamide / urea	Absorption peak of O-H groups / cm^{-1}	Force constant /10^{-21} N/m
Native starch	-	3531.69	-
FUTPS	10/1/2	3513.08	5.19
	10/2/1	3456.70	20.75
	10/2/2	3457.27	20.59
	10/3/1	3458.54	20.24

According to Eq. (1) and (2), Δf was calculated in Table. 3. The kind and content of plasticizer had strong effect on Δf of O-H group in TPS. When the mass proportion of formamide to urea changed from 1/2 to 2/1, the wave number of group O-H in TPS moved 56.38 cm^{-1} toward the lower frequency. The total content of compound plasticizer was same, but Δf of O-H group had great changes. It could be regarded as the control experiment. One of them refers to the FUPTPS (10:1:1) adding one part formamide and the other refers to FUPTPS (10:1:1) adding one part urea. The first mentioned of two has an evident influence on the wave number of O-H group. Therefore, it was testified that formamide molecular was easier to combine with starch molecules and formed the stronger hydrogen bonds than urea. Also, formamide had better plasticized effects. The oxygen in formamide-urea compound plasticizer molecular acted as a hydrogen bond donor and the receptor was hydrogen in starch molecular, which formed new strong hydrogen bonds and weakened the hydrogen bonds existed in starch molecules. With the total content of compound plasticizer increasing (from 30~40%)，the absorption peaks of group O-H remained at 3457 cm^{-1} and Δf of O-H group had few changes. Hydrogen bonds were obtained between plasticizer molecules instead of starch molecules. Excessive amounts of plasticizers obstructed the normal molecular combination and reduced the efficiency of weakening hydrogen bonds in the starch molecules. Therefore, the appropriate content of plasticizer should be chosen to plasticized starch.

There were amino groups in formamide and urea molecules. Thus, an absorption peak appeared at 1687.18cm^{-1} in Fig.3. Amino groups could form hydrogen bonds (N-H···O) with the starch molecules, and hydrogen bonds (N-H···O) were more stable and stronger. Plasticization made the starch chains unordered and the starch was able to be processed easily.

3.2 DSC analysis

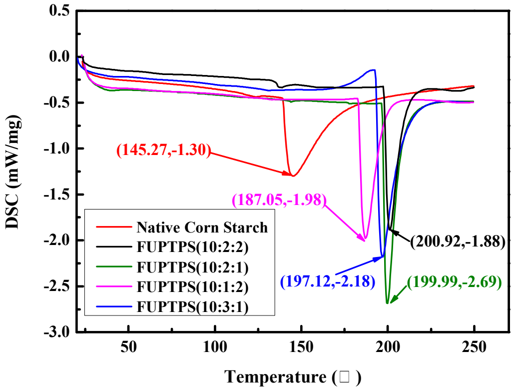

Fig. 4 DSC curves of native starch and FUTPS

DSC analysis of native starch, and TPS samples was shown in Fig. 4. In the temperature range (20-130℃), DSC curves showed a decreasing trend, but the rate of dropping is very slow. This is attributed to the depolymerization reaction of few glucosyl groups with the temperature increasing. As temperature was increased successively, absorption peaks appeared in Fig. 4, which indicated thermal cracking of starch.

In Fig. 4, peak temperature (Tp) of the crystal melting transition was respectively 145.27, 187.05, 197.12, 199.99 and 200.92◦C. The temperature of thermal cracking of TPS was significantly higer than the native starch. These proved that plasticization could increase the melting temperature of starch. With the melting point of starch increasing, the problem was solved that the glass transition temperature of starch was closely to its melting temperature. Therefore, the heat stability and processability of starch was improved to some extent. The temperature interval of hydrogen bonds between starch molecules and fiber hydroxyls was improved, which had significant effects on mechanical properties of the composites. Besides, no significant effect on the melting point of TPS with excessive amounts of plasticizers was observed in Fig. 4.

3.3 X-ray analysis

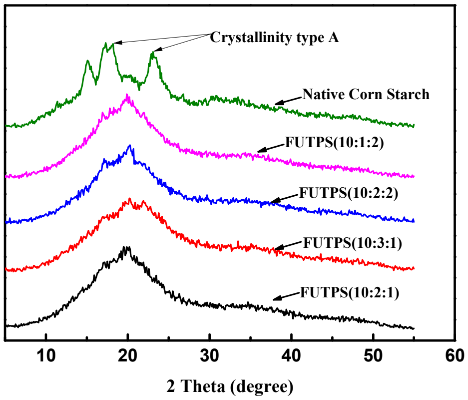

Fig.5 X-ray diffractograms of native corn starch and FUTPS

The recorded XRD patterns for native starch and FUTPS were depicted in Fig. 5. The results demonstrated important changes in the structure of the starch after plasticization. The analysis of the native corn starch displayed a predominance of crystallinity type A. And diffraction peaks of native corn starch locate at 2θ=15.1°, 18°, 23.1°. After processing with the formamide-urea plasticizer, the change in the crystalline structure of starch was clearly visible in the X- ray diffractograms. The crystalline order observed in the native starch granules is completely destroyed in TPS, The formation of B- and V-type crystalline structures occurred because of the recrystallization of starch. Therefore, it was indicated that the plasticizers molecules obstructed the forming of the hydrogen bonds between the starch molecules and formed new hydrogen bonds with starch molecules. Besides, the restraint of the crystallization could lead to improvement of mechanical properties of the TPS composites accordingly.

3.4 Infrared spectrum analysis on composites

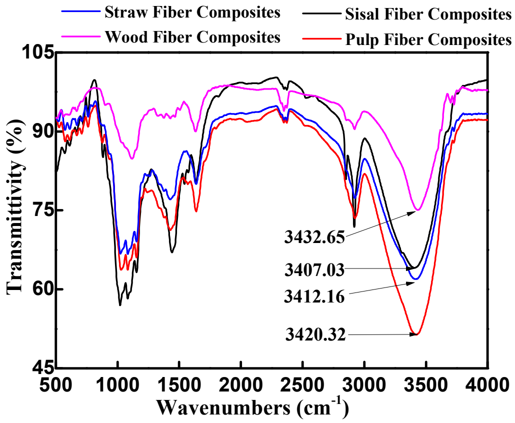

Fig. 6 The infrared spectra (FTIR) of four kinds of fibers reinforced composites

The thermoplastic starch from native corn starch was obtained by plasticization with the optimum plasticizing proportion (2:1) of formamide-urea compound plasticizers. Sisal, pulp, straw and wood were used as fiber reinforcement to prepare thermoplastic starch matrix composites. The IR spectroscopy investigations of different fibers composites were shown in Fig.6. The wave number of O-H groups were respectively, 3407.03cm^{-1}(sisal fiber composites), 3420.32cm^{-1}(pulp fiber composites), 3412.16cm^{-1}(straw fiber composites) and 3432.65cm^{-1}(wood fiber composites), which were all less than 3531.69cm^{-1}, the minimum wave number of thermoplastic starch in Fig.3. The hydrogen bonds in the composites became stronger after the mould foaming process.

When analyzing FTIR spectra in Fig.6, it was found that the influence of types of fibers on the hydrogen bonds through O-H groups were evident. Due to the decomposition of the compound plasticizers during mould foaming process, the hydrogen bonds in thermoplastic starch were broken and became free hydroxyls. The cellulose, a long carbon-chain polymer in the treated fibers, also had great amounts of hydroxyls. As the mould foaming progressed, the exposed hydroxyl groups attracted mutually to form a new hydrogen bonds between the fiber macromolecular chain and thermoplastic starch chain. These hydrogen bonds were more stable and stronger and overcame the problem that natural fibres were unbonded with the starch. Fibers presented a disordered state, which promoted their own overlapping in the formation of hydrogen bonds. Hence, the wave number and absorbance of composites moved towards the low frequency in Fig. 6 and the interactions by hydrogen bonds were stronger.

During the mould foaming process, the compound plasticizers occurred decomposition at high temperature. Hence, the N-H···O groups would not be discussed in this section.

As shown in Fig. 6, compared to three other fibers composites, the absorption peaks of O-H groups in sisal fiber composites were minimum, and the displacement towards lower frequency was maximum. It indicated that the intermolecular hydrogen bonds between sisal fiber molecular and thermoplastic starch molecules were the strongest. Therefore, it was concluded that the mechanical properties of sisal fiber composites were better than the other three fibers composites, which had been verified in the following mechanical properties experiment.

3.5 Thermogravimetric analysis

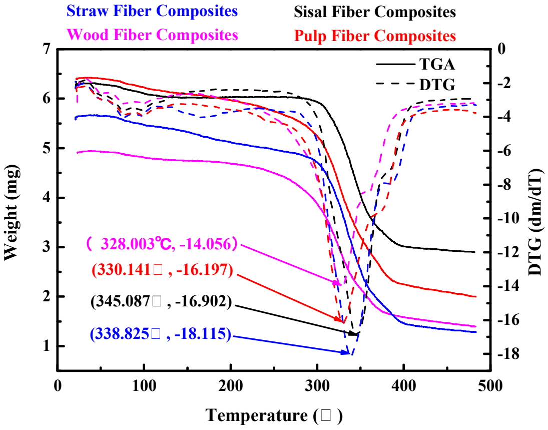

Fig. 7 TG and DTG curves of four kinds of fibers reinforced composites

Thermogravimetric analysis (TGA) was performed on the composites, where the mass loss due to the volatilization of the degradation products was monitored as a function of temperature. The thermogravimetric (TG) and derivative thermogravimetric (DTG) curves of different fibers reinforced composites were shown in Fig. 7. TG curves showed a decreasing trend before the onset temperature, but the rale of dropping is very slow. This mass loss was related to the volatilization of water, formamide and urea in the composites. The decomposed temperature, Tmax was the temperature at maximum rate of mass loss in TG, i.e. the peak temperature in DTG. The degradation of straw, sisal, wood and pulp fiber composites took place at 338, 345, 328 and 330◦C, respectively. The thermal stability of the sisal fbier composites was best among the test samples. It was related to the better thermal stability of sisal fiber and the best interaction between fiber and starch matrix shown in Fig. 7.

3.6 Mechanical properties tests.

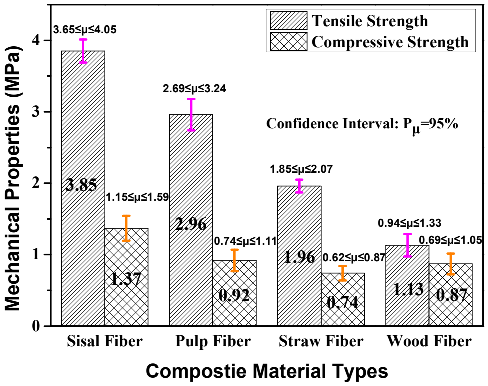

Fig. 8 The tensile and compressive strength of four kinds of composites

Fig. 8 showed the results of tensile strength and compressive strength tests on four fibers reinforced biomass composites. The tensile strength from large to small was listed as sisal fiber, pulp fiber, straw fiber and wood fiber reinforced biomass composites. Two reasons explained that why sisal fiber reinforced biomass composites had the highest tensile strength. One was that the intermolecular hydrogen bonds were the strongest between plant fiber molecular chains and thermoplastic starch molecules in the four kinds of biomass composites. The other was that the tensile strength of sisal fiber itself reached 600MPa.[19] The length of treated wood fiber was too short to form the space network structure in the biomass composites. Although the cost of wood fiber was high, the tensile strength of wood fiber composites was lowest.

In Fig.8, the compressive strength of sisal fiber composites was superior to other fibers with reinforced composites. It was mainly because the fibers formed the space network structure during mould foaming process, and the good cell structure could effectively increase the compressive strength of the composites.

3.7 The analysis on SEM

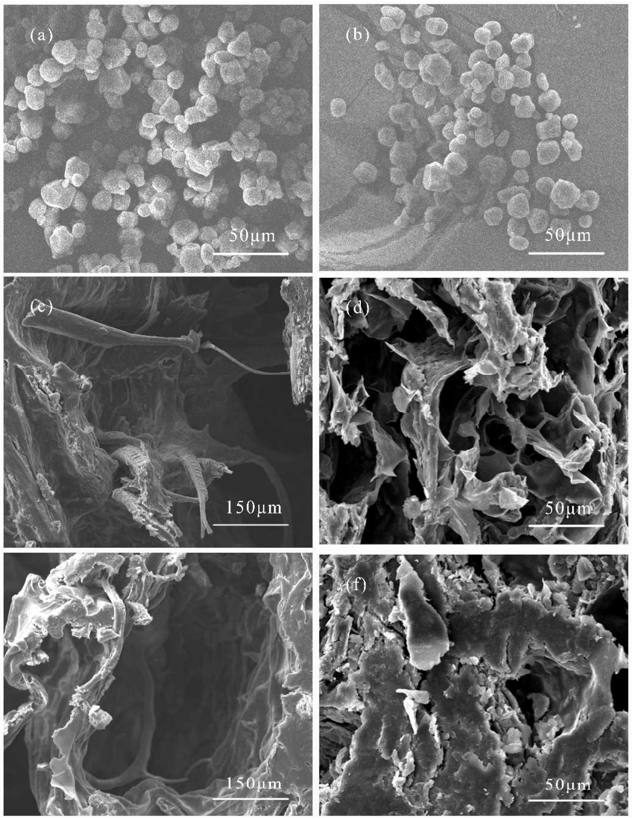

Fig. 9 SEM images (a) native corn starch; (b) thermoplastic starch; (c) sisal fiber composites; (d) pulp fiber composites; (e) straw fiber composites; (f) wood fiber composites;

Fig.9 (a) and Fig.9 (b) were the contrast figures of starch before and after plasticizing. Compared to the Fig.9 (a), plasticization disrupted the crystal structure of starch. And the molecular structure was disordered and decentralized in the Fig.9 (b). As a result, plasticized starch obtained better thermoplasticity and hydrophilicity and was easier to combine with other molecules.

In Fig. 9, SEM images of biomass composites, (c) sisal fiber, (d) pulp fiber, (e) straw fiber, (f) wood fiber were showed. It was clearly observed that the fibers were bonded with starch like reinforced concrete construction. Besides, reticular structure was formed in the composites. Composites of Fig.9 (c) were made from thermoplastic starch and sisal fibers. The fracture surface showed the broken fibers. Just like the reinforced concrete construction, the properties of concrete reinforcing bars were determined by the strength of the concrete construction. Similarly, the strength of the fibers was closely related to the performances of composites. Sisal fibers were long and thick with better tensile strength. So, the sisal fiber composites had better cell structures and mechanical properties. This ratiocination was demonstrated by the analysis of Fig. 8. The fracture surface of pulp fiber composites was shown in Fig. 9 (d), where scrobiculate structure was presented. This reticular formation was an ideal microscopic structure and always demonstrated preferable mechanical properties. TPS and pulp fibers adhered well, forming space grid structure with uniform foam cell. Although pulp fibers had the worse properties than three other kinds of fibers, the pulp fibers composites with scrobiculate structures showed the better mechanical performances in Fig. 8. Due to the high cost of pulp fibers, it was not often chosen as the main material to prepare the composites. The straw fiber composites in Fig.9 (e) adhered with starch well and had good cell structure. But the foam cells were not dense. In addition, the straw fibers were fine and crisp. So, the straw fiber composites demonstrated poor mechanical performances. In Fig.9 (f), the crumb structure was obtained instead of the space grid structure for wood fiber composites. Therefore, the wood fibers were not the appropriate reinforcements for the mould foaming composites.

4. Conclusions

Starch plasticization can effectively destroy the crystal structure of native starch, increase the melting point of starch and improve the processability. When the mass ratio of starch/formamide/urea is 10/2/1, the starch would get the best plasticized effect. Formamide is superior to urea in starch plasticization based on the analysis of hydrogen bonds. Besides, excessive amounts of plasticizers obstructed the normal molecular combination and reduced the efficiency of weakening hydrogen bonds in the starch molecules.

The hydrogen bonds in the composites become stronger after the mould foaming process. Those new hydrogen bonds between the fiber macromolecular chain and thermoplastic starch chain are the main physical interactions, which determine the space grid structure and the mechanical performances.

Compared to three other fibers composites, sisal fiber composites obtain the most stable hydrogen bonds, the best thermal stability and the best mechanical properties, with tensile strength of 3.85MPa and compressive strength of 1.37MPa.

Sisal, pulp and straw fiber composites can form the good space grid structure with better foaming effect. Besides, the wood fibers were not the appropriate reinforcement for composites obtained by mould foaming process. Sisal fiber composites will become the focus of future research with good foaming structure and better mechanical properties.

This research laid a foundation for the analysis of physical interactions in starch plasticization and composites and would benefit any future research on natural fiber-reinforced thermoplastic starch biomass composites.

This work was financially supported by the National Natural Science Foundation of China No. 51305239, the Natural Science Foundation of Shandong Provincial No. ZR2013EEQ010, China Postdoctoral Science Foundation funded project No. 2013M531591, and Postdoctoral Innovation Project of Shandong Provincial No. 201202018. We would like to thank colleagues from Shandong University.

Notes and references

School of Mechanical Engineering & Key Laboratory of High Efficiency and Clean Mechanical Manufacture (Ministry of Education), Shandong University, Jinan 250061, China

*Authors to whom correspondence should be addressed,
Fax: +86-531-88396436;
Tel: +86-13805310890;
E-mails: lifangyi2006@gmail.com

1 J.C. Pei. *China Light Industry Press: Beijing, China*, 2012; **pp**. 198.
2 T. Mekonnen, P. Mussone, H. Khalil, D. Bressler. *Journal of Materials Chemistry A*, 2013, **1(43)**, 13379.
3 J.L. Guimaraes, F. Wypych, C.K. Saul, L.P. Ramos. *Carbohydrate Polymers*, 2010, **80,** 130.
4 N. P. G. Suardana, Y. Piao, J. K. Lim, *Materials Physics and Mechanics*, 2011, **11(1)**, 1.
5 B. Jurca, A. Tirsoaga, A. Ianculescu, O. Carp. *Journal of Thermal Analysis and Calorimetry,* 2014, **115(1)**, 495.
6 Y. Xie, P. R. Chang, S. Wang, J. Yu, X. Ma. *Carbohydrate Polymers,* 2011, **83(1)**, 186.
7 G. Li, F.Y. Li, K.K. Guan. *Journal of Functional Materials*, 2013, **13(44)**, 1969.
8 G. Li, F.Y. Li, N. Xie, K.K. Guan, P. Liu, J.F. Li. *Advanced Materials Research,* 2013, **750-752**, 1239.
9 M. Thunwall, A. Boldizar, M. Rigdahl. *Biomacromolecules*, 2006, **7**, 981.
10 W.Y. Qiu, X.H. Qiu, J.W. Yu, Z.Y. Deng, Q. Xiao. *Transactions of the Chinese Society of Agricultural Engineering,* 2008, **24**, 185.
11 M. E. Vallejos, A. A. S. Curvelo, E. M. Teixeira, F. M. Mendes. *Industrial Crops and Products,* 2011, **33**, 739.
12 J. L. Wang, F. Cheng, P. X. Zhu. *Carbohydrate Polymers*, 2014, **101**, 1109.
13 V. P. S. Nykänen, O. Härkönen, A. Nykänen, P. Hiekkataipale, J. Ruokolainen, O. Ikkala. *Green Chemistry,* 2014, **16(9)**, 4339.
14 A. Donnadio, M. Pica, M. Taddei, R. Vivani. *Journal of Materials Chemistry*, 2012, **22(11)**, 5098.
15 Z.Q. Fu, L.J. Wang, H. Zou, D. Li, B. Adhikari. *Carbohydrate Polymers*, 2014, **101**, 727.
16 K. Naka, R. Yamashita, T. Nakamura, A. Ohki, S. Maeda, K. Aoi, M. Okada. *International Journal of Biological Macromolecules*, 1998, **23(4),** 259.
17 A. Pawlak, M. Mucha. *Thermochimica Acta*, 2003, **396(1)**, 153.
18 S.F. Weng. *Chemical Industry Press: Beijing, China,* 2012; **pp**. 39.
19 H. Feng, L.J. Wang. *Science Press: Beijing, China*, 2010; **pp**. 180.